

HYDROGEN AUTOIGNITION IN A TURBULENT DUCT FLOW: EXPERIMENTS AND MODELLING

E. Mastorakos*, C. Markides

Y. M. Wright

Department of Engineering, University of
Cambridge

LAV-IET, ETH Zurich

*Corresponding author: Trumpington Street, Cambridge CB2 1PZ, UK. Email:
em257@eng.cam.ac.uk

ABSTRACT

This paper presents experimental data on the autoignition of hydrogen jets in a turbulent co-flow of hot air and associated modelling using the Conditional Moment Closure. The aim is to understand better how turbulence affects autoignition of non-premixed flows and to validate modelling approaches. It is demonstrated that the turbulent mixing causes randomness in the ignition location, that it can delay the onset of autoignition and that the autoignition time has a higher sensitivity to temperature than that expected in homogeneous mixtures. The CMC method successfully reproduces the measured autoignition times.

Key Words: autoignition, turbulent, CMC

NOMENCLATURE

d	[m]	fuel nozzle diameter
D	[m]	tube diameter
D_t	[m^2/s]	turbulent diffusivity
L	[m]	ignition spot axial location
L_t	[m]	turbulence lengthscale
N	[$1/s$]	conditional scalar dissipation
Q	[-]	conditional mean
P	[-]	pdf of mixture fraction
T	[K]	temperature
u'	[m/s]	turbulent velocity fluctuation
U	[m/s]	air bulk velocity
Y	[-]	mass fraction
r	[m]	radial coordinate, from tube axis
x	[m]	axial coordinate, from exit of nozzle

h, x	[-]	mixture fraction
c	[$1/s$]	unconditional scalar dissipation

Subscripts and Superscripts

a	air stream
j	fuel (jet) stream

1. INTRODUCTION

The effect of turbulence on autoignition of inhomogeneous mixtures is a topic of fundamental importance in turbulent combustion and of practical relevance in diesel and Homogeneous Charge Compression Ignition engines and in lean-premixed prevapourised gas turbines. The development of these novel combustion technologies is limited by the capability to predict the behaviour of the slow reactions leading to autoignition in the presence of inhomogeneities. In the past, DNS has revealed that ignition occurs at a "most reactive" mixture fraction and at spots with low scalar dissipation rates [1-4]. However, these findings have not been confirmed experimentally and the effect of turbulence intensity and lengthscale on ignition time has not been clarified. In addition, the connection between the ensemble-mean behaviour (for example the average ignition timing measured from many cycles in a diesel engine) and the possibility of relatively rare events causing occasional dangerous autoignition (e.g. in a gas turbine premix duct) has not been explored. In an effort to understand these phenomena better and to provide practically-relevant information on ignition times in the

presence of turbulence and scalar gradients, a turbulent autoignition flow rig has been built and is described in Section 2. In parallel, a modelling effort with the Conditional Moment Closure that has been used in the past for autoignition problems [5-6], is made to assist interpretation of the data and to examine the structure of autoignition zones (Section 3). The results are presented and discussed in Section 4. The paper closes with a summary of the most important conclusions.

2. EXPERIMENTS

The apparatus is shown in **Figure 1**. Air at atmospheric pressure is heated electrically at a temperature T_a up to 1100 K and flows with velocities U_a up to 40 m/s through a perforated plate with 3 mm holes in a 1 m long quartz pipe of inner diameter $D=25$ mm. Fuel (at present H_2 , pure or diluted with N_2) is injected axially and continuously through a $d=2.5$ mm ID stainless steel nozzle. For most of its length, the nozzle is encased in a ceramic pipe of 2 mm thick walls to insulate the fuel from the hot air. The nozzle is located about 50 mm from the perforated plate to allow the turbulence to develop. Images of OH chemiluminescence are taken with an ICCD camera (LaVision Nanostar) fitted with a Nikon UV lens and an interference filter band-centred at 307 ± 10 nm. The images are taken with an exposure time of 0.2 ms. The air temperature is measured 10 mm before the injector with an R-type thermocouple corrected for radiation and conduction loss. Measurements further downstream showed that the temperature is uniform for radii up to about $r=10$ mm for all axial locations where data are presented in this paper, but decreases sharply towards the walls. Heat losses are reduced by thick lagging around the quartz tube with an opening about 200 mm long for optical access. The velocity is also uniform across the pipe up to $r/D=0.4$, as found from pitot-tube measurements under hot conditions ($T_a=850$ K). Under cold conditions, hot-wire measurements showed very thin boundary layers at the wall of the duct and the turbulence intensity was about 10% with the turbulence lengthscale about 2.1 mm. Therefore we may conclude that the air flow is essentially uniform across the pipe in terms of velocity, turbulence and temperature.

Despite the insulation of the nozzle, the exit temperature of the fuel, T_f , has been found to be high, but less than T_a . By extensive measurements

at T_a slightly lower than those needed for ignition, a simple analysis for heat transfer across the nozzle was validated. This was subsequently used to calculate T_f when ignition occurs and the temperature at the injector cannot be measured. The range of T_f so calculated is between 550 and 650 K.

The method of rig operation and ignition length measurement is as follows. Once the rig has reached thermal equilibrium after about one hour of operation, the required flow rate of air is set and a small flow of N_2 is passed through the fuel nozzle to keep it cool. Then the fuel is switched on and mixes with nitrogen upstream of the nozzle and final adjustments to the flow rates are made. The dilution of the fuel stream is described by the mass fraction of hydrogen, $Y_{fu,0}$, which is 0.13 for all data shown here. Once the system has reached its final equilibrium, about 100 images of OH chemiluminescence are taken with the ICCD. The images are then processed by removing background noise by setting the intensity as zero below a certain threshold. The highest level of amplification is then enforced to the image so that the light intensity takes essentially everywhere either a zero or the maximum value. Hence, the presence of OH would result in a normalized unity signal, while the absence of OH in zero. The presence of OH is deemed as an ‘‘autoignition spot’’. The individual images are then used to compile the probability density function of the spot’s location, from which the mean $\langle L \rangle$ and the r.m.s., L_{rms} , are calculated.

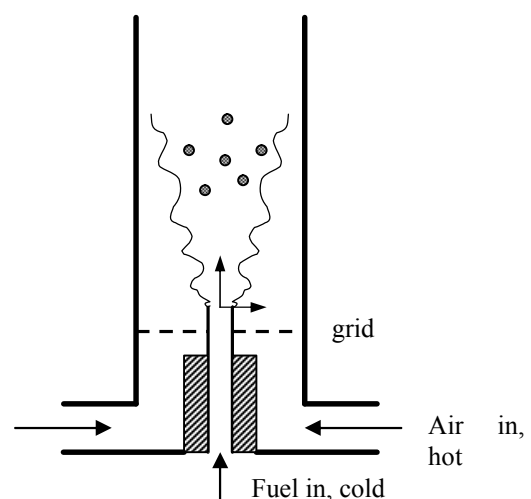


Figure 1. Schematic of the experimental arrangement.

3. MODELLING

The first-order Conditional Moment Closure coupled with the commercial CFD solver STAR-CD is employed for modelling this experiment. Solutions of the velocity field and of the mean and variance of the mixture fraction without combustion are obtained with STAR-CD with an axisymmetric grid of 50x100 nodes in the radial and axial direction respectively. The solutions from the CFD code are then passed to a code solving the CMC equations, described next.

The CMC method [7] aims to describe how the conditionally-averaged reactive scalars depend on the mixture fraction, a conserved scalar. The resulting equations are partial differential equations in 5 dimensions (t, x, y, z, \mathbf{h}) . In generic form, the modeled CMC equations can be written as

$$\frac{\partial Q}{\partial t} + C_j \frac{\partial Q}{\partial x_j} = \frac{\partial}{\partial x_j} \left[D_t \frac{\partial Q}{\partial x_j} \right] + \langle N | \mathbf{h} \rangle \frac{\partial^2 Q}{\partial \mathbf{h}^2} + S(\mathbf{h}) \quad (1)$$

where the coefficient C_j describes convection, D_t is the turbulent diffusivity, and $\langle N | \mathbf{h} \rangle$ the conditional scalar dissipation rate. These are functions of physical and mixture-fraction space and contain information from the fluid mechanical field. The Favre-averaged velocity, turbulent diffusivity, mean and variance of the mixture fraction, and the unconditional scalar dissipation rate ($\tilde{u}_j, D_t, \tilde{\mathbf{x}}, g^2, \tilde{c}$ respectively) come from the CFD solution. The source term $S(\mathbf{h})$ contains the chemistry. Closure is performed here at first order. The chemistry is hence calculated by CHEMKIN subroutines using the conditionally-averaged mass fractions and temperature. Second-order corrections to account for any conditional fluctuations have also been developed [5,7], but not used here. A model for the conditional velocity term and the Girimaji model for the conditional scalar dissipation rate [7] are employed. Once the Q 's are known, the Favre-averaged species and temperature can be found by integrating over a presumed pdf of the mixture fraction, taken as a beta-function. For more details, see Refs. [6-7]. The chemical mechanism is from Ref. [8] and has been validated for laminar counterflow hydrogen autoignition concerning the limiting temperature for ignition as

a function of strain rate and hence is suitable for the present work.

The CMC equations are discretised by finite differences and this leads to the construction of a large number of o.d.e.'s. These are then integrated with the package DVODPK, which can handle very large systems of stiff equations, and hence no splitting between real space, \mathbf{h} -space and chemistry is necessary. For the present problem, we neglect axial diffusion but we keep the cross-stream diffusion of the conditional averages in order to account for the heat losses to walls and the different scalar dissipation rate across the jet that may affect the autoignition behaviour. A grid with 101 nodes in \mathbf{h} -space and 51 nodes in the radial direction is employed.

4. RESULTS AND DISCUSSION

4.1 Bulk behaviour

Visual observations at different operating conditions showed the following. At high T_a and low U_a and U_j , as soon as the fuel is switched on, autoignition and subsequent flashback occurs. The first appearance of ignition is randomly located in space and flashback occurs with what seems like a triple flame (**Fig. 2, a**) and results in a normal jet diffusion flame. This is the “flashback” regime. For a certain range of lower T_a , higher U_a or high dilutions, a statistically-stable situation is observed where autoignition occurs at random spots at about 5-50 d from the injector (**Fig. 2, b,c,d**). These spots result in neither flashback nor act as flame anchoring points, but are short-lived ignition kernels that die out. This is the “random spots” regime. For even lower T_a or higher U_a , no ignition is observed in the observation section of the pipe, although occasional ignition can be heard from further downstream. Ignition completely disappears as T_a decreases further. We call this the “no ignition” regime. The “random spots” regime produces an intense noise with decreasing pitch as the temperature decreases. The boundary between the “flashback” and the “random spots” regime is quite sharp. **Figure 3** shows that a higher temperature is needed to cause flashback at high fuel jet velocities, but this temperature decreases with air velocity. More data are necessary to map out accurately the regime boundaries. However, the main features outlined here have been observed under a wide range of velocities and with other fuels too (e.g. acetylene). The ignition location as a

function of air temperature and velocity and fuel jet velocity for the “random spots” regime is described in more detail next, where the boundary between this and the “no ignition” regime is also discussed.

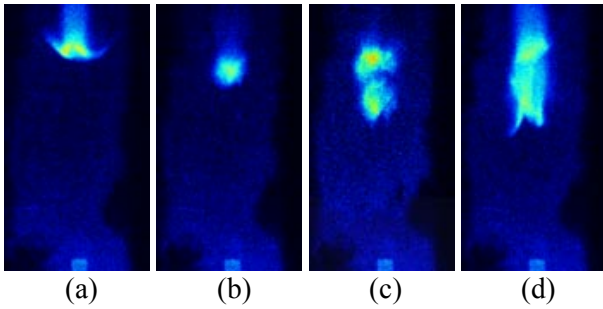


Figure 2. Examples of raw OH chemiluminescence images. $U_a=26\text{m/s}$, $T_a=1000\text{K}$, $U_j=63\text{m/s}$, $Y_{fu,0}=0.13$ for (b), (c), (d); Same, but $T_a=1050\text{K}$ for (a), which shows a flame propagating towards the injector.

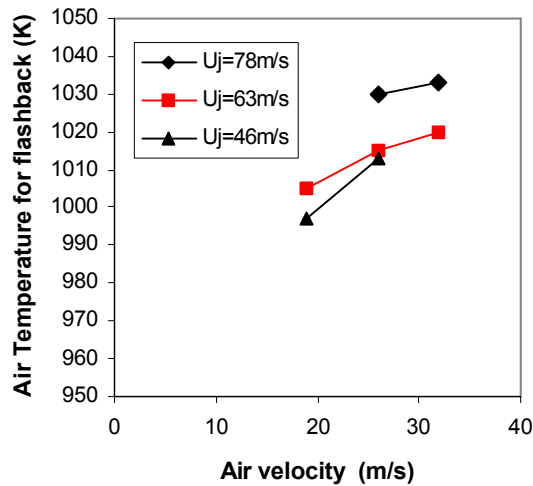


Figure 3. The air temperature required to cause flashback as a function of air velocity.

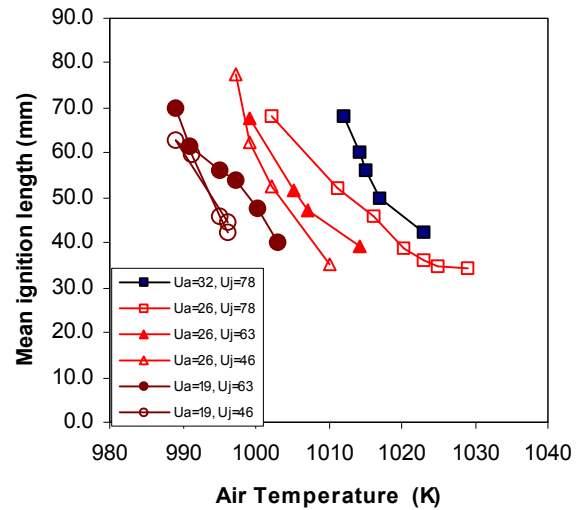


Figure 4. Mean ignition lengths based on images such as that of Fig. 2 as a function of air temperature for different air and jet velocities.

4.2 Ignition length

From the OH images, the statistics of the location of the autoignition spot can be compiled. The mean values for various conditions are shown in **Figure 4** as a function of the air temperature. The ignition location shifts downstream with decreasing T_a , increasing U_a or increasing U_j . The trends are non-linear and the ignition length increases sharply as the temperature decreases, which explains why the boundary between the “no ignition” and the “random spots” regimes is not well-defined. In contrast, for every one of the curves shown, flashback would occur for a temperature higher than the last point shown by about 2-3 K, which shows that the boundary between the “random spots” and the “flashback” regime is sharper (Fig. 3). The same conclusions can be drawn if the ignition length is defined as the *minimum* axial location seen for an OH spot. This minimum length is about 30% shorter than the mean shown in Fig. 4.

The randomness of the autoignition spot location can be quantified with the r.m.s. of the length and this is given in **Figure 5**. It is evident that the r.m.s. is large and this is attributed to the turbulence. The ratio $L_{rms}/\langle L \rangle$ increases with the air temperature, but seems to be independent of air and fuel velocities.

The present data can assist the development of theoretical models for autoignition. For example, since the pdf of ignition location has been measured, calculations with transported pdf

methods can be verified in detail [9]. Further measurements of velocities and temperature, as well as high-speed visualization are under way to assist understanding of the statistical nature of autoignition in this flow.

4.3 Ignition times

A mean residence time until the point of ignition could be defined simply as $\langle L \rangle / U_a$. However, this does not take into account the velocity of the jet, which can be a factor of two or three higher than the air velocity. In addition, many of our data show ignition at close distances to the nozzle and hence the jet momentum cannot be ignored. A better definition of residence time can be made based on a mean velocity U^* , given by

$$t = \frac{\langle L \rangle}{U^*} = \int_0^{\langle L \rangle} \frac{dx}{U(x)} \quad (2)$$

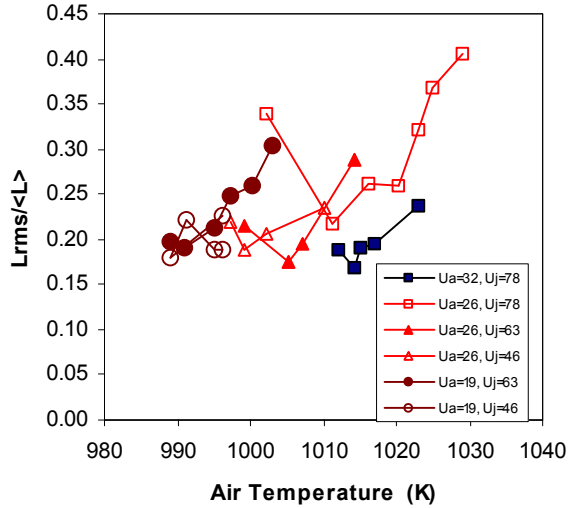


Figure 5. The r.m.s. divided by the mean ignition length from images such as Fig. 2. Same data as in Fig. 4.

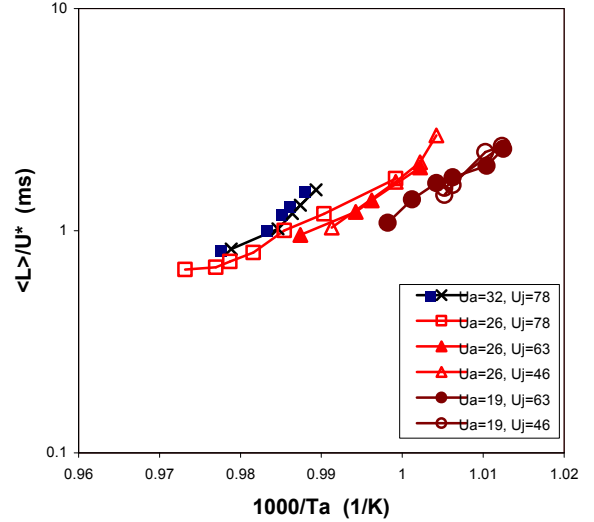


Figure 6. The data of Fig. 4 processed to give an ignition time according to Eq. (2).

with $U(x)$ being the centreline velocity of the jet. This can be found from experimental data. For jets in turbulent co-flows with comparable velocities, the normalized axial centreline velocity has been correlated with $(U(x) - U_a) / (U_j - U_a) = F(x / d_{eff})$ where $d_{eff} = d \sqrt{\mathbf{r}_j / \mathbf{r}_a}$. The densities of both streams can be found from their known composition and the measured T_a and the estimated T_f , while the function F from Ref. [10]. The residence times until the point of ignition hence defined are shown in **Figure 6**. It is evident that the data for different jet velocities collapse approximately on a single band, while the curves with different air velocities do not. This was also evident from a straightforward use of $\langle L \rangle / U_a$ and also from using the minimum lengths rather than the mean (not shown). It can be concluded that the mean residence time until the point of ignition increases with air velocity. This suggests that the phenomena are not simply kinetically controlled, but that the turbulence and mixing must play a role in determining the location of autoignition. The fact that at the same T_a a higher air velocity results in later autoignition, suggests a delaying effect of the air stream on ignition. It is possible that the higher air speed results in higher scalar dissipation rates, which in turn delay autoignition. Further measurements of the mixture fraction and the turbulence characteristics, as well as tests with different turbulence promoting grids, must be

performed to understand better and verify these observations.

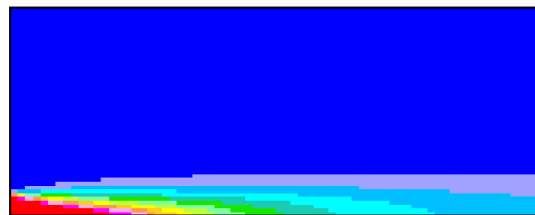
Figure 6 can also be considered as an Arrhenius plot and hence can be used to define an effective activation energy. Focusing on each data set (i.e. ignition time as a function of T_a for the same U_a and U_j), the slopes so defined range from 38000K to 70000K. This activation temperature decreases with increasing jet velocity. These values are higher than those found in uniform hydrogen-air mixtures: experimental data at 1 bar [11] shows an activation temperature about 30000 K at the same temperature range, while predictions at 50 bar [12] give an activation temperature of 22000 K. It is also evident that the Arrhenius plots are not straight lines and that they depend on the velocity. The data do not span a wide enough range to draw solid conclusions, but it seems that a single activation temperature cannot be defined. Turbulent mixing can cause non-linearity in Arrhenius plots [2] and hence the present data suggest that the pre-ignition reactions have been influenced by the turbulence. However, this conclusion must be re-examined with other fuels that show a less complex kinetic behaviour than hydrogen where thermal feedback may not be a prerequisite for autoignition [8].

4.4 CMC predictions

The CFD predictions confirm that over the length of interest here, the mean velocity, turbulence and temperature remain approximately uniform across the central part of the tube. However, once the thermal boundary layers growing at the walls meet, the centreline temperature begins to decrease quickly, in agreement with the measurements. **Figure 7** shows that the fuel plume is slender because in these flows, where the jet and the co-flow have velocities that do not differ much, it is the background air turbulence that causes mixing and the plume is hence expected to grow more slowly than a jet in a quiescent environment. **Figure 8** shows that the Favre-averaged temperature (calculated from the conditional averages and subsequent integration over the presumed mixture fraction pdf) decreases due to heat losses close to the walls. This is captured because the CMC equations include a spatial diffusion term. Before ignition, the hot air mixes with the cold fuel. Ignition occurs at $t=1.9\text{ms}$. Following that, the whole of the central part of the flow is burning. In mixture fraction space, ignition always occurs at the “most reactive”

mixture fraction [1-2] $x_{MR}=0.03$ for the present conditions (**Figure 9**), but this does not imply that the spatial location of ignition will be where the *mean* mixture fraction assumes this value. For example, the first ignition in Fig. 8 (at $t=1.9\text{ms}$) corresponds to a mean mixture fraction of 0.35 and a second (independent) ignition event occurs at $t=2.0\text{ms}$ and at $\tilde{x}=0.08$. The fact that CMC includes a physical space dependence is important. Figure 9 shows that the conditionally averaged fuel mass fraction has decreased for x_{MR} at the point of ignition, but is still at its inert value at other spatial points. The spatial diffusion term causes flame spreading across the jet, which results in the high temperatures of Fig. 8 at late times.

In **Figure 10**, the CMC predictions are compared with the data and it can be concluded that the model reproduces satisfactorily the ignition times. Different turbulence parameters (intensity, lengthscale) are also tested and it is evident that the autoignition time is predicted to depend on these. This occurs mostly through their effects on the mixing field (Fig. 7), which in turn changes the conditional scalar dissipation. In addition, if the temperature is low enough that autoignition would occur after the thermal boundary layer has reached the centre of the flow, autoignition will be delayed further and may even be precluded. The calculations of Fig. 10, if plotted as an Arrhenius plot, show an activation temperature about 50000 K, which is higher than the 25000 K found from calculations of homogeneous mixtures with the same mechanism in the same temperature range. Hence the observed sensitivity to temperature is not simply of kinetic origin, but is due to the fact that high scalar dissipation rates delay ignition. Despite the uncertainty in the experimental definition of ignition time and in the specification of the turbulence parameters, we may conclude that the elliptic CMC model captures many of the observed features of hydrogen autoignition in a turbulent duct flow.



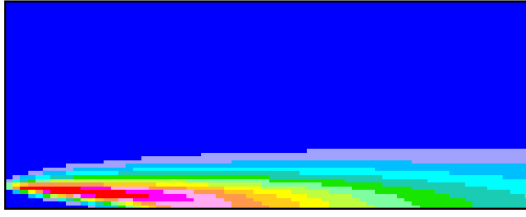


Figure 7. Contours of the mean (upper; spanning 0 and 1) and the variance (lower; spanning 0 and 0.18) of the mixture fraction. Fuel enters from the lower left corner.

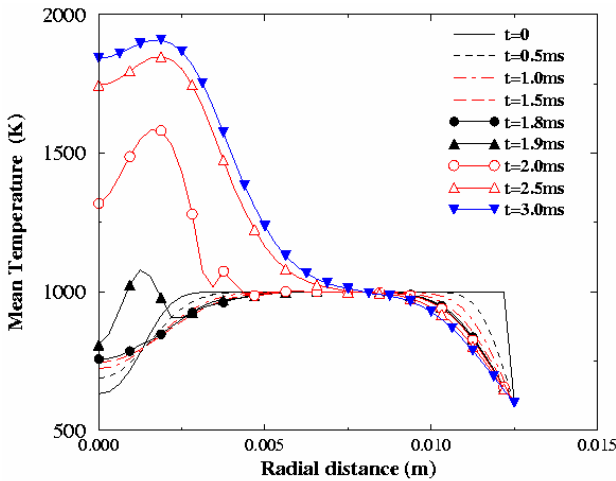


Figure 8. The Favre-mean temperature across the jet at different times (defined as x/U_a). $U_a=26\text{m/s}$, $U_f=46\text{m/s}$, $T_a=1000\text{K}$, $T_f=628\text{K}$, $Y_{fu,0}=0.13$.

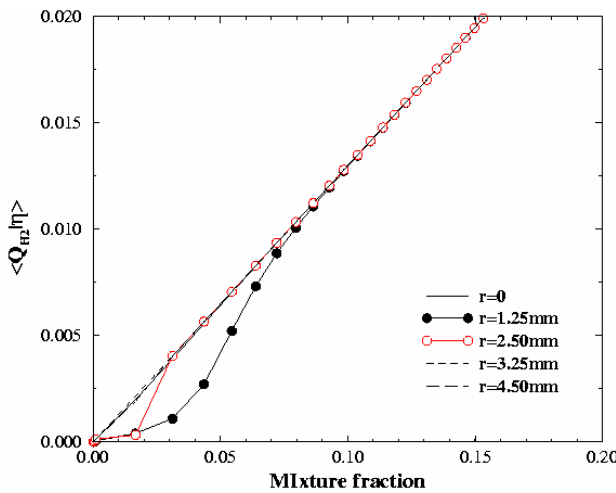


Figure 9. The conditional fuel mass fraction as a function of mixture fraction immediately after autoignition for various radial locations. Conditions as in Fig. 8.

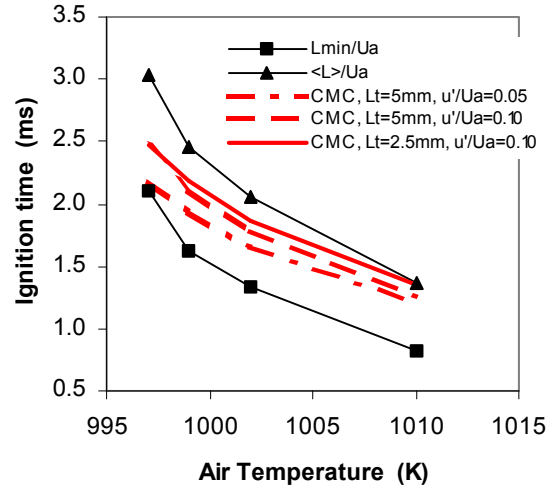


Figure 10. Comparison of predicted with measured ignition times for different time definitions and input air turbulence intensities and lengthscales. For all, $Y_{fu,0}=0.13$, $U_a=26\text{m/s}$, $U_f=46\text{m/s}$, and $T_f=628\text{K}$.

5. CONCLUSIONS

The autoignition of nitrogen-diluted hydrogen jets in a fast turbulent co-flowing stream of hot air has been studied experimentally and computationally. The experiment shows that there is a regime of temperatures and velocities where a statistically-steady situation is reached with autoignition occurring in randomly-located spots. The mean ignition length derived from measuring the OH chemiluminescence from these spots increases as the air or fuel velocities increase or as the temperature decreases. A calculation of the mean residence time until the point of ignition shows that the ignition time at the same temperature increases with increasing air velocity, an observation that suggests that the present data are not simply kinetically controlled, but that the turbulence delays autoignition. Arrhenius plots also show a non-linearity, which further suggests effects of mixing on autoignition. Modelling with the Conditional Moment Closure reproduces the experimental data satisfactorily and reveals the structure of the autoignition zone. In the future, more refined measurements will be undertaken to compile data for model validation and different fuels will be tested to verify the present conclusions.

ACKNOWLEDGMENTS

This work has been partly funded by the European Commission through programs PLANET and STOPP.

REFERENCES

- [1] Mastorakos, E., Baritaud, T.B. & Poinso, T.J., 1997a, "Numerical Simulations of Autoignition in Turbulent Mixing Flows", *Combust. Flame*, vol. 109, pp. 198-223.
- [2] Mastorakos, E., Pires da Cruz, A., Baritaud, T.B. & Poinso, T.J., 1997b, "A Model for the Effects of Mixing on the Autoignition of Turbulent Flows", *Combust. Sci. and Tech.*, vol. 125, pp. 243-282.
- [3] Hilbert R. & Thevenin, D., 2002, "Autoignition of Turbulent Non-premixed Flames Investigated Using Direct Numerical Simulations", *Combust. Flame*, vol. 128, pp. 22-37.
- [4] Sreedhara, S. & Lakshmisha, K.N. (2000) "Direct Numerical Simulation of Autoignition in a Non-premixed, Turbulent Medium", *Proc. Combust. Inst.*, vol. 28, pp. 25-34.
- [5] Mastorakos, E. & Bilger, R.W., 1998, "Second-order Conditional Moment Closure for the Autoignition of Turbulent Flows", *Phys. Fluids*, vol. 10, pp. 1246-1248.
- [6] Kim, S.H., Huh, K.Y. & Fraser, A.R., 2000, "Modeling Autoignition in Turbulent Methane Jet by the Conditional Moment Closure Method", *Proc. Comb. Inst.*, vol. 28, 185-191.
- [7] Klimenko, A.Y. & Bilger, R.W., 1999, "Conditional Moment Closure for Turbulent Combustion", *Prog. Energy Combust. Sci.*, vol. 25, pp. 595-687.
- [8] Kreutz, T.G. & Law, C.K., 1996, "Ignition in Nonpremixed Counterflowing Hydrogen versus Heated Air: Computational Study with Detailed Chemistry", *Combust. Flame*, vol. 104, pp. 157-175.
- [9] Lakshmisha, K.N., Rogg, B. & Bray, K.N.C., 1995, "PDF Modeling of Autoignition in Nonpremixed Turbulent Flows", *Combust. Sci. and Technol.*, vol. 105, pp. 229-243.
- [10] Sakai, Y., Watanabe, T., Kamohara, S., Kushida, T. & Nakamura, I., 2001, "Simultaneous Measurements of Concentration and Velocity in a CO₂ Jet Issuing into a Grid Turbulence by Two-Sensor Hot-Wire Probe", *Int. J. Heat and Fluid Flow*, vol. 22, pp. 227-236.
- [11] Bozhenkov, S.M., Starikovskaia, S.M. & Starikovskii, A. Yu., 2003, "Nanosecond Gas Discharge Ignition of H₂ and CH₄ Containing Mixtures", *Combust. Flame*, vol. 133, pp. 133-146.
- [12] Bradley, D., Morley, C., Gu, X.J. & Emerson, D.R., "Amplified Pressure Waves During Autoignition: Relevance to CAI Engines", SAE Paper 2002-01-2868.